Correlative Studies of Gating in Cx46 and Cx50 Hemichannels and Gap Junction Channels

Miduturu Srinivas,* Jack Kronengold,† Feliksas F. Bukauskas,† Thaddeus A. Bargiello,† and Vytas K. Verselis†
*Department of Biological Sciences, State University of New York College of Optometry, New York, New York; and †Department of Neuroscience, Albert Einstein College of Medicine, The Bronx, New York

ABSTRACT Transjunctional voltage (V_j) gating of gap junction (GJ) channels formed of connexins has been proposed to occur by gating of the component hemichannels. We took advantage of the ability of Cx46 and Cx50 to function as unapposed hemichannels to identify gating properties intrinsic to hemichannels and how they contribute to gating of GJ channels. We show that Cx46 and Cx50 hemichannels contain two distinct gating mechanisms that generate reductions in conductance for both membrane polarities. At positive voltages, gating is similar in Cx46 and Cx50 hemichannels, primarily showing increased transitioning to long-lived substates. At negative voltages, Cx46 currents deactivate completely and the underlying single hemichannels exhibit transitions to a fully closed state. In contrast, Cx50 currents do not deactivate completely at negative voltages and the underlying single hemichannels predominantly exhibit transitions to various substates. Transitions to a fully closed state occur, but are infrequent. In the respective GJ channels, both forms of gating contribute to the reduction in conductance by V_j. However, examination of gating of mutant hemichannels and GJ channels in which the Asp at position 3 was replaced with Asn (D3N) showed that the positive hemichannel gate predominantly closes Cx50 GJs, whereas the negative hemichannel gate predominantly closes Cx46 GJs in response to V_j. We also report, for the first time, single Cx50 hemichannels in oocytes to be inwardly rectifying, high conductance channels ($\gamma = 470$ pS). The antimalarial drug mefloquine, which selectively blocks Cx50 and not Cx46 GJs, shows the same selectivity in Cx50 and Cx46 hemichannels indicating that the actions of such uncoupling agents, like voltage gating, are intrinsic hemichannel properties.

INTRODUCTION

Functional channels composed of connexins include undocked or unapposed hemichannels as well as cell-cell or gap junction (GJ) channels. The finding that hemichannels can function when unapposed was originally described for Cx46 (Paul et al., 1991; Ebihara and Steiner, 1993), but has now been demonstrated for several other connexins (White et al., 1999; Zampighi et al., 1999; Valiunas and Weingart, 2000; Contreras et al., 2003).

Both connexin GJ channels and unapposed hemichannels are regulated by voltage. GJ channels, which have been more widely studied, have been shown to gate in response to transjunctional voltage, V_j, the voltage difference between cells (see Harris, 2001; Bukauskas and Verselis, 2004). For homotypic GJ channels that are formed by the docking of identical hemichannels, junctional conductance, g_j, is typically maximum when the cells are at the same potential, i.e., at $V_j = 0$, and declines symmetrically with V_j values of either polarity. Symmetry in gating about $V_j = 0$ in GJ channels has been attributed to the fact that gating occurs in the component hemichannels. Because of head-to-head docking, the hemichannels are positioned in opposite orientations along the transjunctional field, thereby generating closure of one hemichannel for one polarity of V_j and the other hemichannel for the opposite polarity.

Recent evidence indicates that there are two distinct voltage-dependent gating mechanisms that can close GJ channels and hemichannels (Trexler et al., 1996; Banach and Weingart, 2000; Bukauskas et al., 2001, 2002). One mechanism closes channels and hemichannels to a subconductance state and has molecular components of its voltage sensor localized to the N-terminal domain, which resides on the cytoplasmic side of the membrane (Verselis et al., 1994; Oh et al., 2000). This form of gating characterized by incomplete closure is responsible for an often reported property of GJs in which steady-state g_j declines to a residual conductance (g_{min}) with increasing V_j. The other mechanism completely closes gap junction channels and hemichannels, leaving no residual conductance, and has a distinctive feature in that the gating transitions appear slow, often taking tens of milliseconds to complete. Molecular components of this form of gating may be at the extracellular end of the hemichannel because of strong sensitivity to extracellular Ca^{2+} (Ebihara and Steiner, 1993; Pfahnl and Dahl, 1999) and resemblance to gating associated with docking during cell-cell channel formation (Bukauskas and Weingart, 1994). The provisional name *loop gating* was assigned because of the plausible involvement of the extracellular loop domains (Trexler et al., 1996).

Consistent with voltage gating being intrinsic to the hemichannels, gating asymmetries of some heterotypic GJs, where the docked hemichannels differ in connexin composition, are predicted by the gating properties of the component hemichannels inferred from the corresponding

Submitted October 7, 2004, and accepted for publication November 29, 2004.

Address reprint requests to Vytas K. Verselis, Dept. of Neuroscience, Albert Einstein College of Medicine, 1300 Morris Park Ave., Bronx, NY 10461. Tel.: 718-430-3680; Fax: 718-430-8944; E-mail: verselis@aecom.yu.edu.

0006-3495/05/03/1725/15 $2.00

doi: 10.1529/biophysj.104.054023

homotypic GJs (for reviews see Harris, 2001; Bukauskas and Verselis, 2004). However, the properties of some heterotypic GJ channels are not predicted in this way, which led to the suggestion that docking can alter or even determine GJ channel gating properties (White et al., 1994). Similarly, studies of unapposed hemichannels have reported gating properties that are both consistent and inconsistent with their docked counterparts. For two related connexins, Cx46 and Cx50, for which gating properties have been reported in both unapposed hemichannels and GJ channels, there are similarities and differences in voltage gating when comparing the two connexins and when comparing undocked and docked configurations of the same connexin. Studies of Cx46 hemichannels at the single-channel level reported gating for both polarities (Trexler et al., 1996), whereas macroscopically, gating only at negative voltages was reported (Beahm and Hall, 2002). The steady-state and kinetic properties of unapposed hemichannels at negative potentials predicted the V_j-dependent reductions in g_j observed in the corresponding homotypic GJ channels (Ebihara and Steiner, 1993; Ebihara et al., 1995), suggesting that Cx46 hemichannels, when incorporated in GJ channels, close at inside negative voltages. However, in heterotypic GJ channels in which Cx46 is paired with Cx26 or Cx32, closure of Cx46 hemichannels was deduced to occur at inside positive voltages (White et al., 1995). For Cx50 hemichannels, there are no single-channel studies of gating that have been reported, but macroscopically there is gating at positive and negative voltages that differs in sensitivity, kinetics, and the extent to which conductance declines compared to Cx46 (Zampighi et al., 1999; Beahm and Hall, 2002). The V_j-dependent reductions in junctional currents observed in homotypic Cx50 GJs matched the steady-state and kinetic reductions in current observed at positive voltages in unapposed Cx50 hemichannels, indicating gating polarity and sensitivity of Cx50 is preserved in hemichannel and GJ channel configurations. This assignment of a positive gating polarity is also consistent with gating properties of heterotypic GJs containing Cx50 (White et al., 1995).

Here we examined gating properties of Cx46 and Cx50 hemichannels expressed in *Xenopus* oocytes, both macroscopically and at single-channel levels. We were able to resolve the discrepancies in the correspondences between gating in unapposed Cx46 hemichannels at macroscopic and single-channel levels and between polarity of V_j-dependent gating in Cx46 and Cx50 GJ channels versus corresponding hemichannels. We also report unitary Cx50 hemichannel currents in *Xenopus* oocytes that are large, with a slope conductance at $V_m = 0$ of 470 pS in contrast to the 32-pS channel previously reported for Cx50 hemichannels in *Xenopus* oocytes (Eskandari et al., 2002). These studies shed light on properties and mechanisms that are intrinsic to hemichannels and how they contribute to the properties of GJ channels.

METHODS

Expression of Cx46 and Cx50 in *Xenopus* oocytes and construction of Cx46 and Cx50 mutants

The coding region of Cx46 was cloned into the *Eco*R1 and *Hin*dIII sites of pGem-7Zf+ (Promega, Madison, WI) from rat genomic DNA using PCR amplification with primers corresponding to amino- and carboxy-terminal sequences. The Cx50 coding sequence was subcloned into the SP64T transcription vector (generously provided by Dr. Thomas White, SUNY, Stony Brook, NY). The Cx46D3N and Cx50D3N mutations were generated using oligonucleotide primers and the polymerase chain reaction. The Cx46D3N and Cx50D3N constructs were subsequently cloned into pGem-7Zf+ and SP64T plasmid vectors, respectively, and sequenced in their entirety. mRNA was prepared from appropriately linearized plasmid DNA with the mMessage mMachine T7 RNA kit from Ambion (Austin, TX), according to manufacturer's protocol. The mRNA was purified using QIAquick PCR purification columns from Qiagen (Valencia, CA). mRNA bound to the column was eluted with 30–40 μl of an aqueous solution of DNA antisense to the endogenous XenCx38 (8 pmol/ml). We used the phosphorothioate antisense oligo 5′-GCT TTA GTA ATT CCC ATC CTG CCA TGT TTC-3′, which is complementary to XenCx38 commencing at NT −5 with respect to the ATG initiation codon. Preparation of *Xenopus* oocytes has been described previously (Rubin et al., 1992). Each oocyte was injected with 50–100 nl of the mRNA/antisense solution. Injected oocytes were kept at 18°C in a standard solution containing 88 mM NaCl, 1 mM KCl, 2 mM $MgCl_2$, 1.8 mM $CaCl_2$, 5 mM glucose, 5 mM HEPES, and 5 mM pyruvate, pH 7.6. Cx50 expression was generally lower than that of Cx46. To achieve comparable levels of current, macroscopic recordings of Cx50 hemichannels were generally obtained 3–4 days after mRNA injection, whereas recordings of Cx46 hemichannels were obtained 1–2 days after injection.

Bath and recording solutions

In macroscopic recordings of hemichannel currents, *Xenopus* oocytes were bathed in a modified ND96 solution containing 88 mM NaCl, 1 mM KCl, 1 mM $MgCl_2$, 5 mM glucose, and 5 mM HEPES, pH 7.6. Appropriate amounts of $CaCl_2$ were added to adjust Ca^{2+} concentrations between 0.2 and 1.8 mM. Both current-passing and voltage-recording pipettes contained 2 M KCl. For patch-clamp recordings of hemichannel currents, *Xenopus* oocytes were manually devitellinized in a hypertonic solution consisting of 220 mM Na aspartate, 10 mM KCl, 2 mM $MgCl_2$, and 10 mM HEPES and then placed in ND96 solution for recovery. Oocytes were then individually moved to the recording chamber containing the patch pipette solution (IPS), which consisted of 140 mM KCl, 1 mM $MgCl_2$, 5 mM HEPES, 1 mM $CaCl_2$, 5 mM EGTA, and pH adjusted to 7.6 with KOH.

Electrophysiological recording of hemichannel currents

For macroscopic recordings of hemichannel currents, *Xenopus* oocytes were placed in a polycarbonate RC-1Z recording chamber (Warner Instruments, Hamden, CT) with a slot-shaped bath connecting inflow and outflow compartments to allow for rapid perfusion. A suction tube was placed in the outflow compartment, and a separate reservoir connected to the main chamber with an agar bridge was used for grounding. Bath volume was ~0.3 ml and total volume exchange was achieved in several seconds by application of solutions to the inflow compartment. At the start of each experiment, oocytes were bathed in a modified ND96. Perfusion solutions consisted of ND96 with reduced amounts of $CaCl_2$ added to adjust Ca^{2+} concentration to 0.2 or 0.4 mM. Mefloquine, generously provided by the Drug Synthesis and Chemistry Branch, Developmental Therapeutics Program, National Cancer Institute (Bethesda, MD), was dissolved in DMSO to give a 100 mM stock and then

diluted in ND96 to final concentrations between 5 and 10 μM. All other chemicals were purchased from Sigma (St. Louis, MO). Flow rates in all experiments were consistent, achieving complete exchange within several seconds. Recordings of hemichannel currents were obtained with a GeneClamp 500 two-electrode voltage-clamp (Axon Instruments, Union City, CA).

For patch-clamp recordings of hemichannel currents, *Xenopus* oocytes were manually devitellinized in a hypertonic solution and then placed in the ND96 solution and allowed to recover for 1–2 h. Oocytes were then moved to a RC-28 recording chamber (Warner Instruments). The bath compartment of the chamber contained the same solution that filled the patch pipettes (IPS solution). The smaller bath compartment was connected via a 3 M agar bridge to a ground compartment. Hemichannel currents were recorded in cell-attached and excised-patch configurations using an Axopatch 1D amplifier (Axon Instruments, Union City, CA). Single hemichannel I-V curves were obtained by applying 8-s voltage ramps from −70 to +70 mV or −160 mV to +50 mV. Single-channel records from voltage steps and ramps were leak-subtracted by measuring leak conductance of a given patch from full closing transitions and extrapolating linearly with voltage. Currents were filtered at 1 kHz and data were acquired at 10 kHz.

Macroscopic and single hemichannel data were acquired using an AT-MIO-16X D/A board from National Instruments (Austin, TX) using our own acquisition software.

Electrophysiological recording and analysis of gap junction (GJ) channels

Recordings of junctional currents between pairs of *Xenopus* oocytes were obtained using the dual two-electrode voltage-clamp technique with two GeneClamp 500 amplifiers (Axon Instruments). At ~24–36 h after injection, oocytes were devitellinized and paired. The procedures used for pairing oocytes and evaluating junctional conductance using the dual voltage-clamp technique have been previously described (Rubin et al., 1992; Verselis et al., 1994). In these experiments, V_j steps were 10 s in duration and applied over a range of ±120 mV in 10-mV increments. Each V_j step was preceded by a small, brief prepulse of constant amplitude (10 mV) so that a family of currents could be normalized if expression levels changed over the course of an experiment. The cells were allowed to recover for 90–120 s between V_j steps. Currents were filtered at 200 Hz and digitized at 1–2 kHz. Initial and steady-state currents were obtained by extrapolating exponential fits of the data to $t = 0$ and $t = \infty$ as previously described (Verselis et al., 1994). Only cell pairs with g_j values ≤ 5 μS were used to avoid effects of series access resistance on voltage-dependence (Wilders and Jongsma, 1992). Data were acquired with an AT-MIO-16X D/A board from National Instruments using our own acquisition software.

RESULTS

Cx46 and Cx50 hemichannel currents in *Xenopus* oocytes

Xenopus oocytes expressing Cx46 in normal external Ca^{2+} concentrations (1.8 mM) exhibited a slowly-activating outward current ascribed to activation of Cx46 hemichannels when stepped to positive potentials, e.g., +40 mV (Fig. 1 *A*). When held at −70 mV, the Cx46 hemichannel current was fully deactivated. Upon lowering external Ca^{2+} to 0.4 mM, the magnitude of the current at positive potentials increased substantially, but still fully deactivated when repolarized to −70 mV, evident by a return to the same holding current as in 1.8 mM Ca^{2+}. In contrast, Cx50 expressing *Xenopus* oocytes in 1.8 mM external Ca^{2+} show little evidence of activation in response to a depolarizing voltage step to +40 mV (Fig. 1 *A*). Lowering external Ca^{2+} to 0.4 mM substantially increased the magnitude of the current at +40 mV, but also increased current at the holding potential of −70 mV. Oocytes expressing Cx50 exhibited outward current that declined from an initial peak to a non-zero steady-state value. Small voltage steps superimposed onto the depolarizing voltage step to +40 mV indicated that the decline in current represented a decrease in conductance consistent with closure of Cx50 hemichannels (data not shown). Upon repolarization to −70 mV, conductance remained high and nearly constant, suggesting that a substantial fraction of Cx50 hemichannels, closed at +40 mV, opened rapidly and largely remained open at −70 mV. These properties attributed to activation of Cx46 and Cx50 hemichannels in *Xenopus* oocytes are qualitatively consistent with previous reports (Ebihara and Steiner, 1993; Trexler et al., 1996; Beahm and Hall, 2002).

Recently it was shown that the antimalarial drug, mefloquine, blocks Cx50 but not Cx46 GJ channels (Cruikshank et al., 2004). We examined whether the observed currents in *Xenopus* oocytes expressing Cx50 or Cx46 hemichannels maintained the same pharmacological distinction. Cx46 hemichannel currents were unaffected by the application of 10 μM mefloquine (Fig. 1 *B*, *left panel*). High sensitivity of Cx46 hemichannels to divalent cations was evident by block with application of a low concentration (10 μM) of zinc. In contrast, 5 μM mefloquine, which was shown to cause nearly complete block of Cx50 GJ channels (Cruikshank et al., 2004), markedly reduced Cx50 hemichannel currents. Block was reversible as currents returned to control levels upon washout (Fig. 1 *B*, *right panel*).

Xenopus oocytes expressing Cx50 displayed a large-conductance channel exceeding 400 pS in symmetric 140 mM KCl. Shown in Fig. 1 *C* are currents of single Cx46 and Cx50 hemichannels obtained by applying ±70 mV voltage ramps. Open hemichannel currents for both Cx46 and Cx50 hemichannels exhibited inward rectification, with currents approximately twofold higher at −70 mV than at +70 mV. Mean slope conductances measured at $V_m = 0$ were 292 ± 11 pS for Cx46 ($n = 25$ ramps, 5 patches) and 469 ± 33 pS ($n = 33$ ramps, 5 patches) for Cx50. As shown below, the different gating properties of the large-conductance channels ascribed to Cx46 and Cx50 account for the differences in the macroscopic properties of currents induced in oocytes expressing these connexins.

Two distinct gating mechanisms are common to Cx46 and Cx50 hemichannels

Gating of Cx46 hemichannels at macroscopic and single-channel levels

When examined at the single-channel level, Cx46 hemichannels were shown to close for both polarities of membrane voltage, with closure to subconductance states at positive

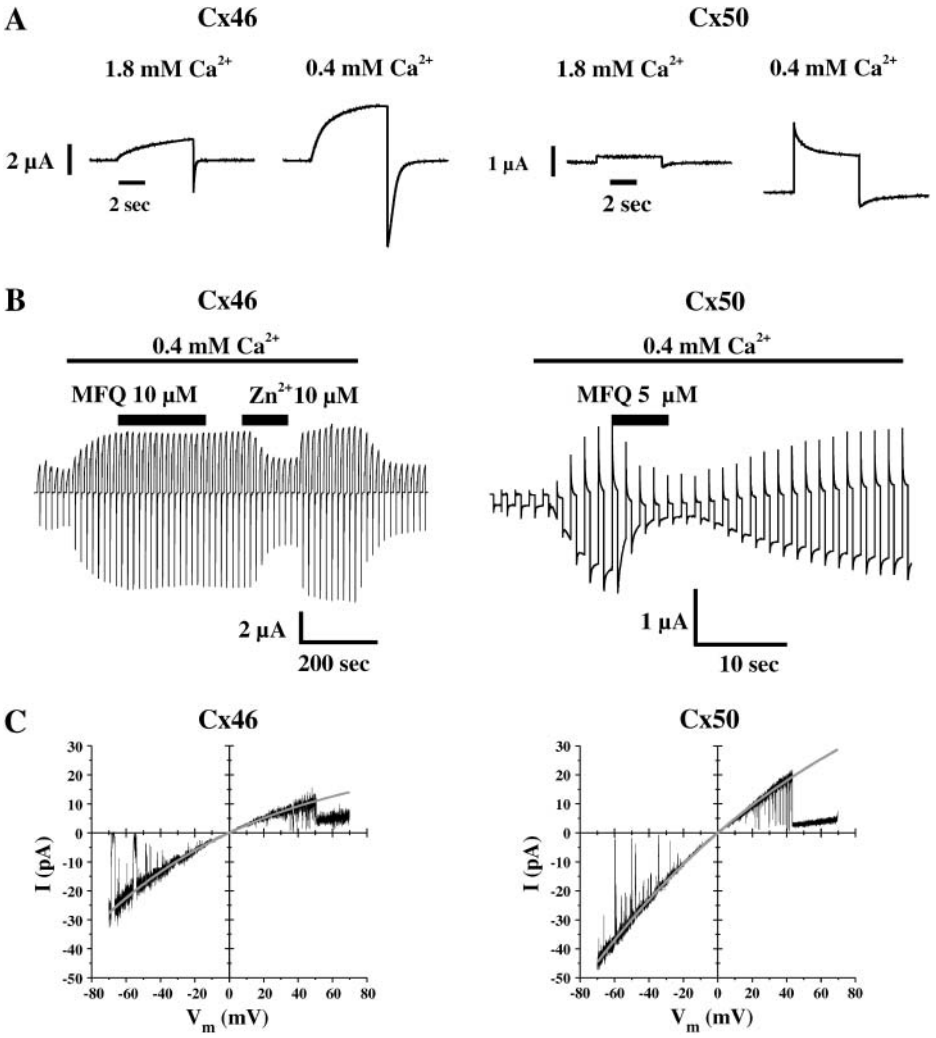

FIGURE 1 Macroscopic and single-channel recordings from *Xenopus* oocytes expressing Cx46 and Cx50. (*A*) Examples of macroscopic currents in oocytes expressing Cx46 (*left panel*) and Cx50 (*right panel*) in normal (1.8 mM) and low (0.4 mM) external Ca^{2+}. In both cases, voltage steps to +40 mV were applied from a holding potential of −70 mV. Cx46 hemichannels activate slowly upon depolarization and close completely upon hyperpolarization. The current magnitude and kinetics of activation are altered upon lowering external calcium. In contrast, Cx50 hemichannel currents showed little activation in normal external calcium. Lowering external calcium caused a large increase in the magnitude of the current at both −70 mV and +40 mV. Mefloquine blocks Cx50 but not Cx46 hemichannels. Mefloquine was applied after hemichannel currents were activated by lowering external Ca^{2+} from 1.8 mM to 0.4 mM. Repeated voltage steps to +40 mV were applied from a holding potential of −70 mV every 15 s. Cx46 hemichannel currents retained sensitivity to divalent cations (10 μM zinc). (*C*) Single-channel currents recorded from an oocyte-patch expressing Cx46 (*left*) and Cx50 (*right*) in response to 8-s voltage ramps from −70 mV to +70 mV. Solid lines represent exponential fits to the open state current. Slope conductance measured at $V_m = 0$ was ~300 pS for Cx46 and ~440 pS for Cx50 in these examples.

voltages and to a fully closed state at negative voltages (Trexler et al., 1996; Pfahnl and Dahl, 1999). These processes were attributed to two different gates, one operating at positive voltages and the other at negative voltages. When examined macroscopically, Cx46 hemichannels were reported to behave differently, with closure evident at negative voltages, but weak or absent at positive voltages (Ebihara et al., 1995; Beahm and Hall, 2002). It is possible that failure to perceive closure of the putative positive gate macroscopically may have been due to the offsetting activation of the negative gate. Therefore, we developed a pulse protocol for macroscopic recordings designed to first open the negative gate of Cx46 hemichannels with a preconditioning pulse before applying a test pulse to a positive voltage. This protocol consisted of a 10-s preconditioning voltage pulse ranging between −40 mV and +80 mV from a holding potential of −70 mV followed by a test pulse to +80 mV. When applied to oocytes expressing Cx46 bathed in 0.2 mM Ca^{2+}, preconditioning pulses between −40 mV and −10 mV, at which there was little opening of the negative gate, resulted in currents during the test pulse that only appeared to activate slowly (Fig. 2 *A*). Preconditioning steps to voltages >+20 mV, which caused substantial opening of the negative gate, resulted in currents during the test pulse that looked very different, showing an initial peak followed by a decline to a non-zero steady-state value. The decrease in current from an initial peak during the test pulse was larger with more positive preconditioning pulses. Examples of currents in response to preconditioning pulses to 0, +10, and +20 mV are shown in an expanded scale. Since elevated external Ca^{2+} has been shown to substantially shift activation of the negative gate of Cx46 hemichannels positive along the voltage axis (Ebihara and Steiner, 1993; Pfahnl and Dahl, 1999), we examined Cx46 currents using the same protocol with oocytes bathed in 2.0 mM Ca^{2+}. A more positive preconditioning voltage pulse was needed to observe a decrease in current in response to the test pulse; compare currents in response to the same three preconditioning pulses shown in the expanded scale (Fig. 2 *B*). These results are consistent with a gate that closes at positive

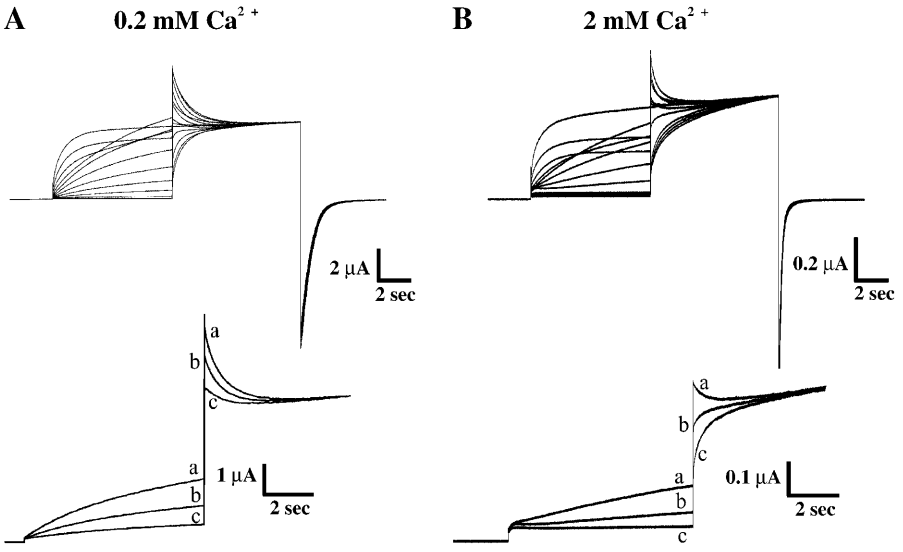

FIGURE 2 Cx46 hemichannels close at inside positive voltages. Examples of macroscopic hemichannel currents recorded from a Cx46-expressing oocyte in external calcium concentrations of 0.2 mM (*A*) and 2.0 mM (*B*). Currents were recorded in response to 10-s conditioning voltage pulses between −40 and +80 mV from a holding potential of −70 mV followed by a test pulse to +80 mV. Reduction of the current during the test pulse, reflecting the gating of Cx46 hemichannels at inside positive voltages, is observed only when currents are first activated during the conditioning pulse. Bottom panels show current traces in response to conditioning voltage pulses of 20 mV (trace *a*), 10 mV (trace *b*), and 0 mV (trace *c*) at expanded scales. In 0.2 mM Ca^{2+}, where there was substantial Cx46 hemichannel activation during the preconditioning voltage steps (traces *a–c* in *A*), application of the test pulse resulted in currents that peaked and declined to a non-zero steady-state value reflecting hemichannel closure. In 2.0 mM Ca^{2+}, where activation is shifted positive, application of a more positive preconditioning pulse was necessary to elicit closure during the test pulse (trace *c* in *B*). At the lower preconditioning voltages of 0 mV and +10 mV where there was little activation, currents during the test pulse appeared to activate slowly.

voltages, whose time course of closure becomes evident when unopposed by concurrent opening of the negative gate. Higher extracellular Ca^{2+} shifts opening of the negative gate to more positive voltages, thereby obscuring the reduction in current over time that accompanies closure of the positive gate.

In Cx46-expressing *Xenopus* oocytes, cell-attached patch recordings using solutions containing Ca^{2+}/EGTA that maintained free Ca^{2+} concentrations below 10^{-7} M exhibited asymmetric gating at positive and negative voltages. In an example of a patch containing several active Cx46 hemichannels, 10-s voltage pulses between −70 and +100 mV applied from a holding potential of −20 mV showed currents that declined to residual values at positive voltages and, in contrast, closed completely at negative voltages (Fig. 3 *A*). Two selected current traces illustrate this polarity-dependent asymmetry in gating. This behavior gives rise to a G_m–V_m relation with a maximum conductance at $\sim V_m = 0$ and reductions for either polarity, characterized by a residual conductance in the positive limb and full closure in the negative limb (Fig. 3 *A*).

In recordings from patches containing a single Cx46 hemichannel (Fig. 3 *B*), virtually all gating at −70 mV consisted of transitions between open and fully closed states that appeared slow, previously shown to be due to transit through a series of transient subconducting states en route to full opening or closure (Trexler et al., 1996; Trexler and Verselis, 2001). This form of gating at negative voltages contrasted that at positive voltages, which consisted of transitions between open and long-lived subconductance states that appeared as rapid, single steps. Full hemichannel closures at positive voltages were rare and if they occurred, were brief, as evident in the recording shown (see Fig. 3 *B*, *arrow*). These results demonstrate agreement between macroscopic and single Cx46 hemichannel currents.

Gating of Cx50 hemichannels at macroscopic and single-channel levels

Macroscopic currents in oocytes expressing Cx50 bathed in 0.2 mM Ca^{2+} in response to voltage steps ranging from +60 to −120 mV applied from a holding potential of −20 mV are illustrated in Fig. 4 *A*. Like oocytes expressing Cx46, those expressing Cx50 exhibit a conductance that is maximal at $V_m = 0$ and declines asymmetrically for positive and negative voltages (see Beahm and Hall, 2002). However, application of a pulse protocol consisting of a test pulse to +60 mV preceded by preconditioning pulses to various voltages produced currents that declined from an initial peak in response to the test pulse regardless of the value of the preconditioning pulse (Fig. 4 *B*). These properties can be explained by considering the same two gates as in Cx46 hemichannels, but with the negative gate in Cx50 hemichannels being largely open at voltages that typically close Cx46 hemichannels. This reduced sensitivity of the negative gate is evident in Fig. 4 *A*, where there was little if any decline in Cx50 current until voltages exceeded −80 mV. Substantial current remained even at voltages as negative as −120 mV. At positive voltages, Cx50 hemichannels behave similarly to Cx46 hemichannels, except for a somewhat higher sensitivity to voltage (reductions in Cx50 currents were observed at voltages as low as +30 mV; see also Beahm and Hall, 2002). These differences in voltage sensitivity at positive and negative

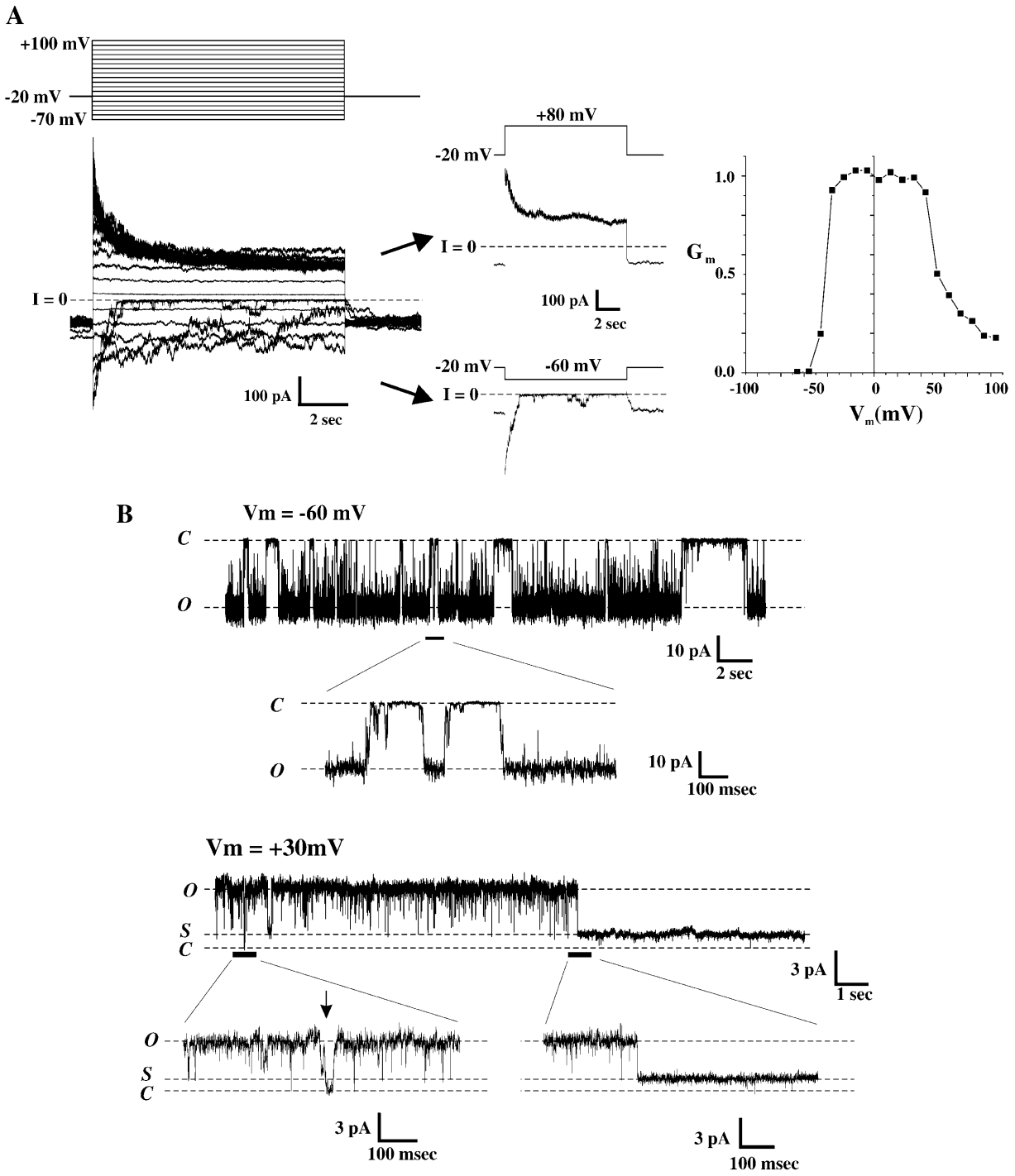

FIGURE 3 Two distinct forms of gating in Cx46 hemichannels. (*A*) Cell-attached patch recordings from an oocyte containing several Cx46 hemichannels. Currents were elicited by applying voltage steps from −70 to +100 mV in increments of 10 mV from a holding potential of −20 mV. Currents peaked and declined to non-zero steady-state values at positive voltages (see selected current trace at +80 mV, *arrow*) and closed completely at negative voltages (see selected current trace at −60 mV, *arrow*). The conductance voltage relationship is asymmetric about V_m=0, reflecting the two distinct types of gating. (*B*) Examples of a single Cx46 hemichannel recorded in the cell-attached mode from an oocyte in response to voltage steps to −60 mV and +30 mV. At −60 mV, single hemichannels predominantly exhibit slow gating transitions to a fully closed state (*C*) from the open state (*O*). In contrast, transitions to a subconductance state (*S*) predominate at positive voltages although brief transitions to the fully closed state are observed. Expanded views at both polarities of regions indicated by the black bars are shown. Single hemichannel recordings are leak-subtracted (see Methods).

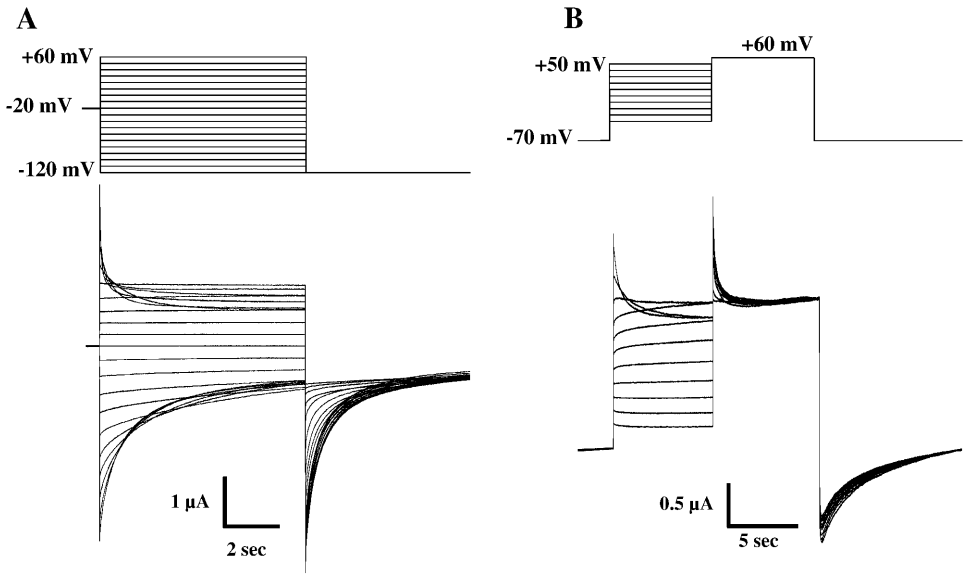

FIGURE 4 Voltage gating of Cx50 hemichannels at the macroscopic level in 0.2 mM Ca^{2+}. (*A*) Macroscopic currents from a Cx50-expressing oocyte showing reductions in conductance at both positive and negative voltages. From a holding potential of −20 mV, voltage steps from −120 mV to +60 mV in increments of 10 mV were applied to this cell. At positive voltages, a decline of Cx50 hemichannel current is evident at membrane potentials as low as +30 mV. At negative voltages, Cx50 currents exhibit little decline until voltages exceed −80 mV; however, even at −120 mV, a residual conductance remains. (*B*) Example of hemichannel currents recorded in response to 10-s conditioning voltage pulses between −40 and +50 mV in 10-mV increments from a holding potential of −70 mV followed by a test pulse to +60 mV. Hemichannel currents decline from a peak to a non-zero steady-state value during application of the test pulse irrespective of the magnitude of the preconditioning pulse. Note that Cx50 hemichannels are largely open at −70 mV; thus depolarizing steps to positive voltages do not cause a large activation of channels as observed for Cx46.

voltages were also evident in macropatch recordings in which external Ca^{2+} concentration was maintained below 10^{-7} M (data not shown, but see single-channel recordings shown below).

In single-channel recordings under conditions where Ca^{2+} concentration was low ($<10^{-7}$ M) Cx50 hemichannels showed a high open probability at small positive voltages (Fig. 5; see traces at $V_m = +10$ mV and +15 mV). At voltages exceeding +20 mV, Cx50 hemichannels frequently closed to long-lasting subconductance states with transitions that appeared as single, rapid steps, reminiscent of gating at the same polarity in Cx46 hemichannels (see current traces at $V_m = +20$, +25, and +30 mV in Fig. 5). Residence times decreased in the open state and increased in subconductance states at higher positive voltages (Fig. 5, see all-points current histograms after each trace). At negative voltages, gating of single Cx50 hemichannels differed markedly from that of Cx46 hemichannels (Fig. 6). Although slow transitions between open and fully closed states were observed, they were infrequent and appeared to exhibit weak sensitivity to voltage. However, Cx50 hemichannels exhibited gating to stable, long-lived substates that increased in frequency with increasingly negative voltages (see traces at −70 and −90 in Fig. 6 *A* and voltage ramps from −160 to +50 in Fig. 6 *B*). The transitions associated with this gating appeared as rapid, single steps in contrast to the slow transitions associated with full closures (see expanded scales, Fig. 6 *A*). Gating to subconductance states at negative voltages in single Cx50 hemichannels explains the incomplete deactivation of Cx50 macroscopic currents at this polarity.

The N-terminal D3N mutation in Cx46 and Cx50 hemichannels abolishes closure at positive voltages

Previous studies have shown that the N-terminus is an integral component of the voltage sensor in GJ channels and that neutralizing the first Asp residue in the N-terminus of Cx32 GJ channels and Cx32*43E1 hemichannels reverses the gating polarity of closure, characterized by transitions to substates leaving the polarity of closure to the fully closed state unaffected (Verselis et al., 1994; Oh et al., 2000). We neutralized the Asp at position 3 in Cx46 and Cx50 by replacing it with Asn (D3N) in attempts to selectively affect the polarity of closure of the positive gate. Unlike hemichannels formed by the respective wild-type connexins, both Cx46D3N and Cx50D3N hemichannels no longer showed reductions in current at positive membrane voltages (Fig. 7, *A* and *B*). However, there were additional and unexpected effects of the D3N substitution (Fig. 7, *C* and *D*). First, unitary conductance was reduced by ~70% in both connexins. Second, gating was significantly altered, in that full closing transitions (characteristic of the negative gate) occurred frequently throughout the voltage range of ±70 mV, indicative of a positive shift in the conductance-voltage relation of this form of gating. These transitions between open and fully closed states were accompanied by frequent brief chirps ascribable to incomplete opening transitions that gave the single hemichannel recordings a ratty appearance. In efforts to better elucidate gating in hemichannels in which D3 was neutralized, we tried additional substitutions in Cx46 such as D3A, D3C, and D3G, but all failed to make

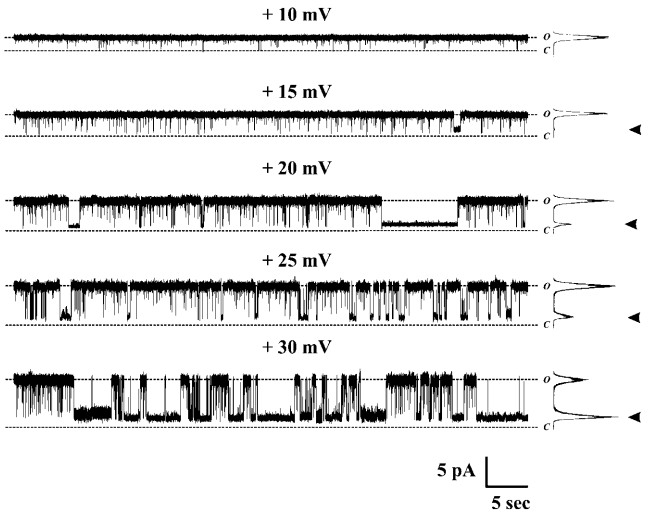

FIGURE 5 Gating of single Cx50 hemichannels at positive voltages. Shown are recordings of single hemichannel currents from a Cx50-expressing oocyte in a cell-attached patch configuration at voltages ranging from +10 to +30 mV. Cx50 hemichannels are predominantly open at low inside positive voltages (see traces at 10 mV and 15 mV). Dwell times in the open state decreased with increasing voltages (see traces at 20, 25, 30 mV), whereas residence in subconductance states were favored at higher voltages. All-points histograms of 60-s recordings are shown to the right of each trace. Arrows indicate the histogram peak assigned to the predominant subconductance state. Full closures were rarely observed and not evident in these recordings. The dotted lines indicate fully open (*O*) and closed (*C*) states. The zero current level was determined as described in Methods.

functional hemichannels. Thus, although the D3N substitution clearly abolished gating at positive potentials in both Cx46 and Cx50 hemichannels, we could not assess whether this result was due to a large shift in sensitivity to voltages beyond those examined, reversal of the polarity of closure, or disruption of the gating mechanism.

Gating in Cx46 and Cx50 GJ channels

Homotypic configurations

The existence of distinct types of gating at positive and negative voltages in unapposed Cx46 and Cx50 hemichannels led us to examine how they contribute to V_j-induced closures in the corresponding GJ channels. Application of V_j steps of either polarity to homotypic Cx46 GJs expressed in pairs of *Xenopus* oocytes gave rise to the steady-state G–V_j relations shown in Fig. 8 *A*. Conductance decreased symmetrically about $V_j = 0$, but did not appear to reach a defined residual conductance, continuing to decline with increasing V_j consistent with previous reports (White et al., 1995; Hopperstad et al., 2000). Interestingly, homotypic Cx46D3N GJs exhibit a G–V_j relation that is nearly identical to that of wild-type Cx46 GJs (Fig. 8 *B*). Since the D3N mutation selectively abolished gating at positive voltages in unapposed Cx46 hemichannels, similarity of the G–V_j relations in Cx46 and Cx46D3N GJs indicates that the negative hemichannel gate is largely responsible for V_j gating in Cx46 GJ channels. For Cx50 GJs, previous reports showed that conductance declined steeply with V_j to a residual conductance (G_{min}) of ~0.2, i.e., 20% of the maximum conductance (White et al., 1995; Srinivas et al., 1999; Beahm and Hall, 2002; Xu et al., 2002). We found that G indeed appeared to decline steeply with V_j to reach a residual conductance of ~0.2 when examined in a V_j range that did not exceed ±70–80 mV (Fig. 8 *C*). The sensitivity of this decrease to the residual conductance resembled that observed in unapposed Cx50 hemichannels at inside positive voltages. However, at V_j values beyond ±80 mV we found a second phase of conductance decrease toward zero. These results indicate that the positive gate of Cx50 hemichannels is largely responsible for closure at V_j values up to ±70–80 mV. At higher V_j values, full closures and/or transitions to substates characteristic of gating of Cx50 hemichannels at negative voltages could give rise to the additional reduction in conductance. Consistent with this explanation, homotypic Cx50D3N GJs no longer exhibited an apparent residual conductance at ±70–80 mV, but rather declined monotonically toward zero (Fig. 8 *D*). Thus, the D3N substitution in Cx50, which abolished gating at positive voltages in unapposed Cx50 hemichannels, abolished gating to the residual conductance in Cx50D3N GJs. In essence, the D3N substitution transforms a Cx50 GJ into one that resembles a Cx46 or a Cx46D3N GJ in which the negative gate, characterized by full closing transitions, is largely responsible for the decrease in conductance with V_j. Gating events at the single-channel level underlying voltage-dependence of homotypic Cx46 and Cx50 GJ channels in transfected N2A cells have been previously reported (Srinivas et al., 1999; Hopperstad et al., 2000; Xu et al., 2002), and lend support to the macroscopic data shown here in *Xenopus* oocytes.

Heterotypic configurations

Pairing Cx46D3N with Cx46 resulted in a GJ with a highly asymmetric steady-state G–V_j relation (Fig. 9 *A*). For voltages relatively negative on the Cx46D3N side, G declined to near zero, whereas for voltages relatively positive, G increased, peaked at $\sim V_j = +50$ mV, and then decreased modestly up to the +120 mV range examined. Pairing Cx50D3N with Cx50 resulted in a junction with very similar characteristics for positive and negative voltages relative to the Cx50D3N side (Fig. 9 *B*). Given the properties of the negative gate observed in Cx46D3N and Cx50D3N hemichannels, the decrease toward zero from the peak conductance is ascribable to closure of this gate in Cx46/Cx46D3N and Cx50/Cx50D3N heterotypic GJs. For voltage relatively negative on the D3N side, the negative gate of D3N hemichannel would dominate, obscuring other gates that close G for this polarity of V_j. For voltages relatively positive on the D3N side (i.e., relatively negative on the wild-type side), reduction in G at high V_j values is ascribable to closure of the negative gate in the corresponding wild-type hemichannels. For Cx46, this is the

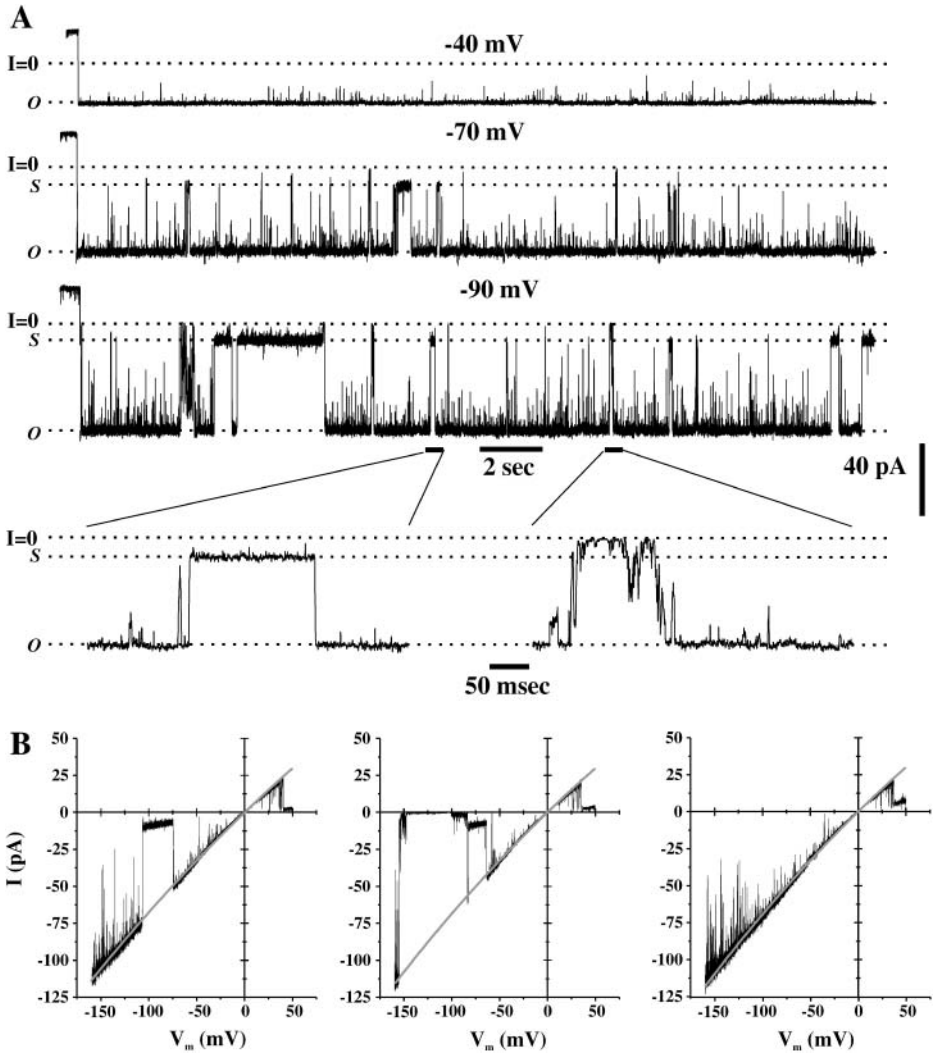

FIGURE 6 Gating of single Cx50 hemichannels at negative voltages. (*A*) Cell-attached patch recordings of single hemichannel activity from a Cx50-expressing oocyte at −40 mV, −70 mV, and −90 mV. Cx50 hemichannels are predominantly open at −40 mV whereas dwell times in the open state decreased with hyperpolarization to −70 and −90 mV. At larger negative voltages, Cx50 channels exhibit two types of transitions, fast transitions between open and subconductance states and slow transitions between the open and closed states (see expanded views showing 500-ms segments indicated by *solid bars*). The dotted line indicates the zero current level. (*B*) Single hemichannel currents obtained with 8-s voltage ramps from −160 mV to 50 mV applied to a cell-attached patch. Shown are three ramps applied in succession, illustrating closing transitions to subconductance and fully closed states. Solid lines represent exponential fits to the open state current.

negative gate that closes Cx46 hemichannels fully and for Cx50 can be either or both of the gating processes observed at negative potentials, one that closes Cx50 hemichannels fully and one that closes hemichannels to substates. The likely basis for the moderate reductions in conductance associated with gating in the respective wild-type hemichannels is discussed below (see Discussion, below).

The similarity of the effects of the D3N substitution on both Cx46 and Cx50 and its dominance in determining the G–V_j relations of GJs is exemplified by the similar characteristics of Cx50/Cx46D3N and Cx46/Cx50D3N heterotypic junctions (Fig. 9, *C* and *D*). The presence of a D3N-substituted hemichannel, whether Cx46D3N or Cx50D3N, results in a very similar G–V_j relation, regardless of whether it is paired to wild-type Cx46 or C50.

DISCUSSION

In this study, we examined two related connexins, Cx46 and Cx50, which readily function as unapposed hemichannels as well as GJ channels when expressed in *Xenopus* oocytes. A number of studies have examined Cx46 hemichannels, both macroscopically and at single-channel levels, and have yielded mixed results as to the correspondence between properties of undocked hemichannels and GJ channels and even correspondence between macroscopic and single-channel properties of Cx46 hemichannels themselves (Ebihara and Steiner, 1993; White et al., 1994; Ebihara et al., 1995; Trexler et al., 1996; Beahm and Hall, 2002). Cx50 has been less widely studied as a hemichannel, but initial investigation of its properties from macroscopic recordings in *Xenopus* oocytes suggested differences in voltage-dependent gating compared to Cx46, particularly at positive voltages (Beahm and Hall, 2002). Here, examination of Cx46 and Cx50 hemichannels, including studies at the single-channel level, shows correspondence between macroscopic and single-channel properties for each connexin and shows that gating in Cx46 and Cx50 differ substantially at negative, rather than at positive, voltages.

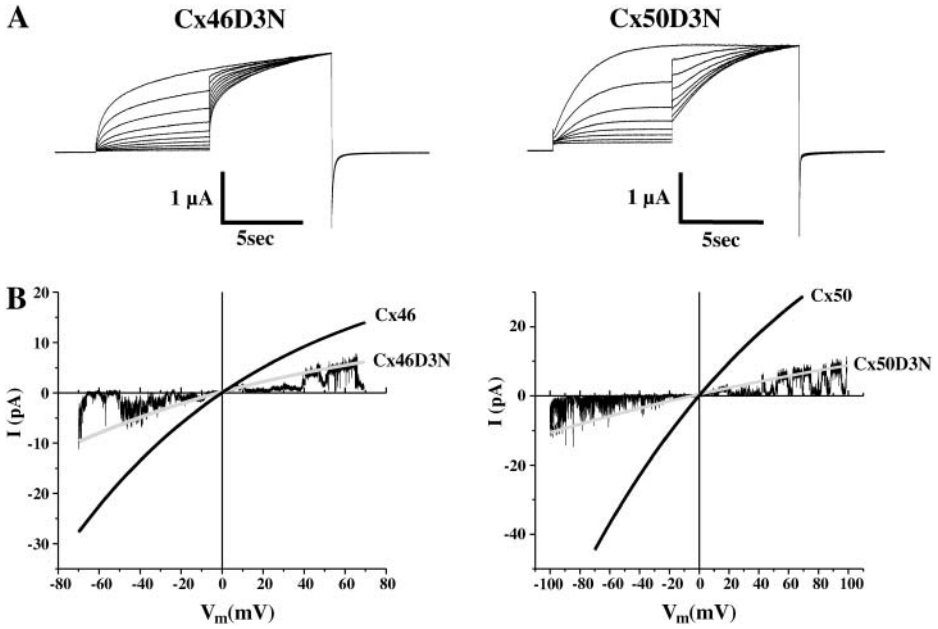

FIGURE 7 The N-terminal D3N mutation in Cx46 and Cx50 hemichannels abolishes closure at positive voltages. (*A*) Examples of macroscopic hemichannel currents recorded from oocytes expressing Cx46D3N (*left*) and Cx50D3N (*right*). Currents were recorded in response to 10-s conditioning voltage pulses between −10 and +80 mV from a holding potential of −70 mV followed by a test pulse to +80 mV. Note that no reduction in currents was observed at positive voltages. (*B*) Single Cx46D3N (*left*) hemichannel and Cx50D3N (*right*) currents were obtained with 8-s voltage ramps from −70 mV to +70 mV applied to cell-attached patches. Shaded lines represent exponential fits to the open state currents. Open state currents of corresponding wild-type Cx46 and Cx50 hemichannels are represented by solid lines. The D3N substitution significantly reduced single-channel conductance and altered gating.

Single open hemichannel properties of Cx46 and Cx50

Unitary conductances of Cx46 and Cx50 GJ channels have been reported to be ~140 pS and ~220 pS, respectively, from dual whole-cell recordings in transfected mammalian cells using pipettes containing 130–140 mM KCl or CsCl salts (Srinivas et al., 1999; Hopperstad et al., 2000; Trexler et al., 2000; Xu et al., 2002). Single open channel I-V relations in

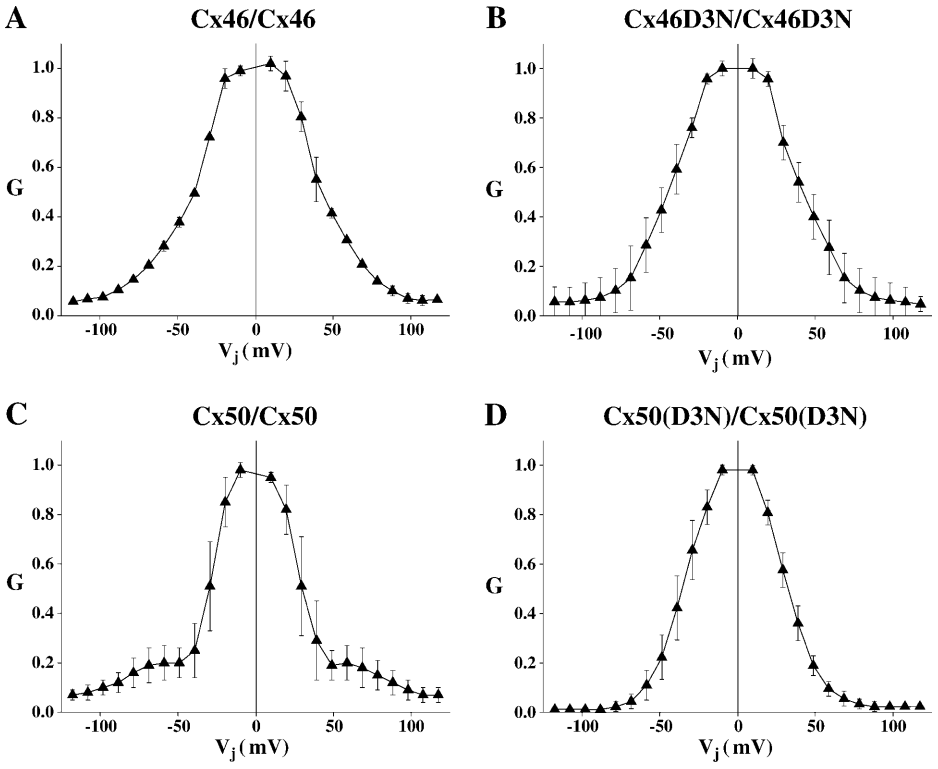

FIGURE 8 Conductance-voltage relationships of homotypic wild-type Cx46 and Cx50 and corresponding homotypic D3N-substituted GJ channels obtained in pairs of *Xenopus* oocytes. In all cases, G is plotted as a function of V_j, where G is G_j/G_{j0}, the conductance normalized to $V_j = 0$, G_j, divided by the normalized initial conductance, G_{j0}. Division of G_j by G_{j0} removes conductance changes due to open channel rectification, leaving changes associated with gating. Positive and negative V_j refers to depolarization and hyperpolarization, respectively, of the same cell of a given cell pair. (*A*) Plot of steady-state G versus V_j for homotypic Cx46 GJs. Steady-state G decreases symmetrically about $V_j = 0$, but does not appear to decline to a plateau nonzero conductance characteristic of most GJ channels. G approaches zero at high V_j values. (*B*) Plot of steady-state G versus V_j for homotypic Cx50 GJs. The G–V_j relationship shows two phases, an initial phase where the conductance decreases steeply with increasing V_j reaching a nonzero plateau at $V_j \sim \pm 70$ mV, and a second phase where the conductance decreases toward zero at higher V_j values. (*C*) Plot of steady-state G versus V_j for homotypic Cx46D3N GJs. The steady-state G–V_j relation is very similar to that of wild-type Cx46. Note that conductance declines toward zero with increasing V_j. (*D*) Plot of steady-state G versus V_j for homotypic Cx50D3N GJs. The G–V_j relation declines symmetrically about $V_j = 0$. However, unlike that of wild-type Cx50, G decreases toward zero, showing no evidence of a residual conductance.

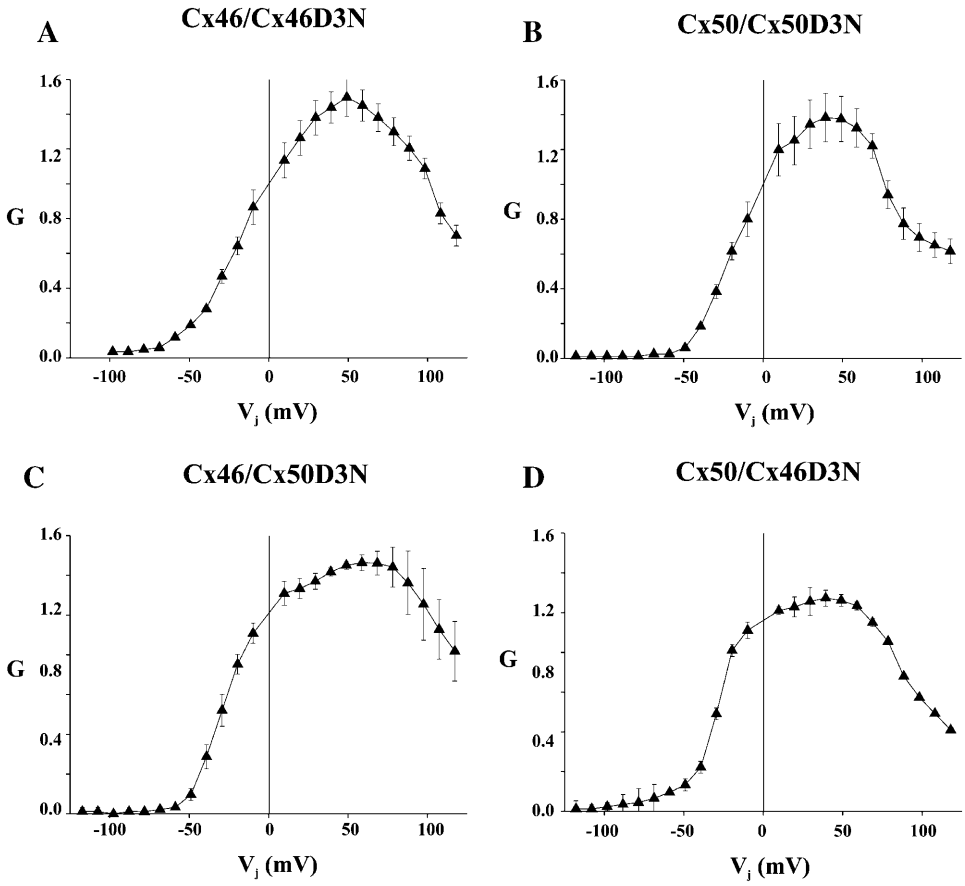

FIGURE 9 Conductance-voltage relationships of heterotypic GJs composed of Cx46D3N and Cx50D3N, each paired to wild-type Cx46 and Cx50 and showing similar properties consistent with dominance of CxD3N hemichannel gating. G is plotted as a function of V_j, with G defined as above in Fig. 8. Positive and negative V_j refers to depolarization and hyperpolarization, respectively, of the cell indicated on the right side of the pairing designation. The panels show plots of steady-state G versus V_j for (*A*) Cx46/Cx46D3N GJs, (*B*) Cx50/Cx50D3N GJs, (*C*) Cx46/Cx50D3N GJs, and (*D*) Cx50/Cx46D3N junctions. In all junctions, G changes asymmetrically about $V_j = 0$, declining to near-zero with V_j relative negative on the D3N side. This result is consistent with closure of the negative gate of the D3N hemichannel in each case. Moderate reductions in G at V_j values relative to positive on the D3N side are consistent with closure of the negative gate in wild-type Cx46 and Cx50 hemichannels.

both cases are linear over a $\pm$70 mV range of V_j. Previous reports have also shown that the single open Cx46 hemichannel I–V relation displays a nearly 2:1 inward rectification over a $\pm$70 mV range of V_m with a slope conductance of $\sim$300 pS at $V_m = 0$ mV, close to twice the conductance of a corresponding GJ channel (Trexler et al., 1996, 2000). A similar conductance for Cx46 hemichannels was reported in transfected HeLa cells (Valiunas and Weingart, 2000). For Cx50 hemichannels, reported unitary conductances are widely disparate, with values of 32 pS reported in *Xenopus* oocytes (Eskandari et al., 2002) and 352 pS in HeLa cells (Valiunas and Weingart, 2000) expressing Cx50. In our hands, patch recordings from *Xenopus* oocytes injected with Cx50 cRNA displayed very large single channels with a slope conductance at $V_m = 0$ of $\sim$470 pS and, like Cx46 hemichannels, a single open hemichannel I-V relation that showed nearly 2:1 inward rectification over a $\pm$70 mV range of V_m. These channels were not observed in uninjected oocytes. Moreover, the properties of these large conductance channels were consistent with those of the macroscopic currents induced in the same Cx50-expressing oocytes.

Fixed negative charges located at the extracellular end, specifically within the first extracellular loop domain, E1, were shown to contribute to the pore and to be important determinants of the high conductance and inward rectifying properties of single Cx46 hemichannels (Trexler et al., 2000; Kronengold et al., 2003). Given the high sequence homology of Cx46 and Cx50 in E1 and throughout the TM domains, it is not surprising that the open hemichannel properties of these two connexins are similar, although the absolute conductance of Cx50 is considerably higher, which likely reflects the presence of an additional fixed negative charge in the Cx50 pore. The difference in conductance between Cx46 and Cx50 GJ channels parallels the difference between Cx46 and Cx50 unapposed hemichannels. Linearity of the single-channel I-V relations of both homotypic Cx46 and Cx50 GJ channels, despite rectifying I–V relations of the corresponding unapposed hemichannels, can be explained by creation of symmetric charge profiles along the pores of the GJs upon head-to-head docking of identical hemichannels. Thus, the open hemichannel properties of both Cx46 and Cx50 hemichannels are in quite good agreement with those expected of half of a GJ channel and indicate that hemichannel pore structure is likely to be minimally different in undocked and docked configurations. Our value of unitary conductance for Cx50 is somewhat larger than the $\sim$350 pS conductance reported in HeLa cells and seemingly incompatible with the $\sim$30-pS conductance reported in *Xenopus* oocytes by Eskandari et al. (2002).

Cx46 and Cx50 hemichannels maintain a differential sensitivity to mefloquine

Recently, quinine and derivatives such as mefloquine were shown to have selective actions on GJ channels formed of different connexin isoforms (Srinivas et al., 2001; Cruikshank et al., 2004). Despite a high primary sequence homology between Cx46 and Cx50, mefloquine potently and selectively blocks Cx50 GJ channels with an $IC_{50} = 1.1\ \mu$M. Concentrations 30- to 50-fold higher have little or no effect on Cx46 GJ channels. Similar selective action was maintained in unapposed Cx46 and Cx50 hemichannels. A quantity of 5 μM mefloquine reduced Cx50 hemichannel currents by ~80%, whereas a higher concentration (10 μM) had no effect on Cx46 hemichannel currents. These data provide additional confirmation that the induced currents in Cx50-injected oocytes are indeed Cx50 in origin. These data also indicate that mefloquine's binding site and action in closing GJs is intrinsic to the hemichannel, consistent with the sidedness of quinine action in heterotypic GJs containing Cx50 (M. Srinivas and D. C. Spray, unpublished results).

Voltage gating in Cx46 and Cx50 hemichannels

In this study, we resolve inconsistencies and discrepancies concerning gating of Cx46 hemichannels at macroscopic and single-channel levels, as well as between gating in Cx46 hemichannels and corresponding GJ channels. We also report differences and similarities between Cx46 and Cx50 hemichannel gating revealed by single-channel recordings.

A large body of evidence from studies of GJ channels in homotypic and heterotypic configurations indicate that gating by V_j is an intrinsic property of the component hemichannels (see Harris, 2001; Bukauskas and Verselis, 2004 for reviews). V_j-dependent properties of heterotypic junctions containing Cx46 or Cx50 suggest a positive gating polarity both for Cx46 and Cx50 hemichannels, i.e., they close with voltages relatively positive on their cytoplasmic sides (White et al., 1995). However, analyses of macroscopic currents from *Xenopus* oocytes showed that unapposed Cx46 hemichannels closed with voltages relatively negative on their cytoplasmic side, and the steady-state and kinetic reductions in Cx46 hemichannel currents at negative voltages correlated with the V_j-dependent reductions in Cx46 GJ currents, presumed to occur at positive voltages (Ebihara and Steiner, 1993; Ebihara et al., 1995). These differences between unapposed Cx46 hemichannels and GJ channels led to the suggestion that Cx46 hemichannels reverse gating polarity upon docking (White et al., 1994). A different situation was reported in Cx50 hemichannels in which the steady-state and kinetic reductions in Cx50 hemichannel currents at positive voltages correlated with the V_j-dependent reductions in Cx50 GJ currents, also presumed to occur at positive voltages (Beahm and Hall, 2002). In the same study, gating of Cx50 hemichannel currents was also observed macroscopically at negative voltages, resulting in asymmetric hemichannel closure at positive and negative voltages, contrasting macroscopic Cx46 hemichannel currents that only appeared to close at negative voltages. Separate studies at the single-channel level, however, showed asymmetric gating for both polarities in Cx46 hemichannels (Trexler et al., 1996).

Discrepancies in the gating properties ascribed to Cx46 and Cx50 hemichannels and GJ channels are resolved by the existence of at least two distinct voltage-sensitive gating mechanisms inherent to the hemichannels. The two gating mechanisms that are common to Cx46 and Cx50, and possibly all connexins, have very distinctive features at the single-channel level. One mechanism is characterized by closures to long-lived substates; the transitions appear as single rapid steps, typical of recordings of gating transitions in most ion channels. In both Cx46 and Cx50, this form of gating closes unapposed hemichannels at inside positive voltages with the probability of closure increasing with depolarization. Sensitivity to positive voltage appears to be somewhat higher in Cx50, although it was not quantified. The other mechanism is characterized by full hemichannel closures with gating transitions that appear slow (10–100 ms) due to transit through a series of short-lived subconducting states (see Trexler et al., 1996). In both Cx46 and Cx50, this form of gating closes unapposed hemichannels at inside negative voltages, but voltage sensitivities differ substantially. Sensitivity is weak in Cx50 hemichannels, but strong in Cx46 hemichannels where it is responsible for the robust and complete deactivation of currents upon hyperpolarization to inside negative voltages. Due to the resemblance of these slow gating transitions to those observed during initial hemichannel docking and formation (Bukauskas and Weingart, 1994), the provisional term *loop gating* was ascribed because of the likely involvement of the extracellular loop domains (Trexler et al., 1996).

In Cx50 hemichannels, since loop gating is weak, what underlies the substantial reduction in current observed macroscopically at inside negative voltages? It turns out to be gating transitions to substates, similar to those observed at inside positive voltages although with a weaker voltage sensitivity. Correspondingly, we see that Cx50 macroscopic currents do not deactivate completely upon hyperpolarization to voltages as high as −120 mV, a finding that differs from that reported by Beahm and Hall (2002) in which Cx50 hemichannel conductance was extrapolated to zero at large negative potentials. This gating behavior is in stark contrast to that of Cx46 hemichannels where only full-closing or loop gating transitions occur at negative voltages. At this point, we cannot distinguish whether the gating transitions to substates at negative voltages in Cx50 represents a third gating mechanism or whether it is related to one of the other two mechanisms. Bipolar gating to substates has been described in some N-terminal mutants of Cx32*43E1 chimeric hemichannels, but the mechanism of bipolar gating remains unclear (Oh et al., 2004).

The reported lack of gating at positive voltages in Cx46 hemichannels when recorded macroscopically can be explained by the interplay between the two gating mechanisms and the dependence of loop gating on Ca^{2+}. Macroscopic currents are typically recorded in solutions containing 1–2 mM Ca^{2+}, where loop gating is shifted along the voltage axis such that Cx46 hemichannels show no evidence of opening until voltages are inside positive. Since both gates are in series, steps to inside positive voltages applied from a negative holding potential do not close the positive gate until the loop gate opens, resulting in a net rise in current that gives the impression that closure at positive voltages does not occur. When preceded by a prepulse that opens a large fraction of loop gates, currents in response to steps to positive potentials exhibit a peak followed by a decline, revealing the time-course of closure mediated by the positive gate. Lowering extracellular Ca^{2+} shifts loop gating to more negative voltages so that closure of the positive gate is visible with steps applied from more negative holding potentials. Since single hemichannel recordings are typically carried out in free Ca^{2+} concentrations below 10^{-7} M, the loop gate would be open at positive voltages and would not interfere with closure of the positive gate, explaining why these gating transitions are always observed in single-channel studies. In Cx50 hemichannels, the two gating mechanisms do not show the same interplay. At the single-channel level, the loop gate is less active in closing Cx50 hemichannels and closure of the positive gate is always observed in macroscopic recordings, even in Ca^{2+}-containing solutions (Fig. 4). This suggests that loop gating is not substantially shifted by external Ca^{2+}. In support, external Ca^{2+} was shown to strongly reduce both Cx46 and Cx50 currents with similar affinities, but the primary action of Ca^{2+} in Cx50 hemichannels did not appear to be a shift in voltage-dependence (Beahm and Hall, 2002). Thus, the action of Ca^{2+} on Cx50 hemichannels may be separate from voltage gating, so that open Cx50 hemichannels respond the same way to voltage in the presence and absence of external Ca^{2+}.

Voltage gating in Cx46 and Cx50 GJ channels

Studies at the single-channel level suggest that the gating mechanisms identified in unapposed hemichannels are also present in GJ channels. For Cx50 GJs, the majority of the gating events in response to V_j are closures to substates via fast transitions and the voltage sensitivity of these gating events matches the steep reduction in g_j to the apparent residual conductance (Srinivas et al., 1999; Xu et al., 2002). The polarity of this gating mechanism deduced from heterotypic pairings is such that the hemichannel on the relatively positive side closes, resulting in correspondence between closure of Cx50 GJ channels and closure of unapposed Cx50 hemichannels at inside positive voltages. Although less frequent, full closures in Cx50 GJs are also observed and can occur from the fully open state or from substates. These events explain the second phase of decline in conductance at higher V_j values. Failure to observe this second phase in other studies may be because of the shorter duration of V_j steps used, and/or to the examination of gating over a smaller range of V_j.

For Cx46 GJs, the majority of the gating events underlying reductions in g_j with V_j are complete closures via slow transitions (Hopperstad et al., 2000). V_j gating events to substates are observed, but are largely obscured by full closures or loop gating. The polarity of loop gating is such that the hemichannel on the relatively negative side closes, which results in correspondence between closure of Cx46 GJ channels and closure of unapposed Cx46 hemichannels at inside negative voltages, just the opposite of that in Cx50. Thus, different gating mechanisms are largely responsible for closing Cx46 GJ channels compared to Cx50 GJ channels. This difference in expression of gating mechanisms is consistent with the results of the D3N mutation, which disrupts gating to substates. In Cx46 GJs, where gating to substates contributes little to the G–V_j relation, the D3N mutation has little effect. In Cx50, where gating to substates is responsible for the majority of the decline in conductance with V_j up to $\pm$70–80 mV, the D3N substitution significantly alters the G–V_j relation, transforming it into one that resembles Cx46 or Cx46D3N.

Although we do not see a defined G_{min} in Cx46 GJs at large voltages due to dominance of loop gating, there is still a small amount of conductance even at $\pm$120 mV (Fig. 8 *A*). Although unapposed Cx46 hemichannels would be closed at these voltages, gating of a Cx46 hemichannel when it is incorporated into a Cx46 GJ channel must consider gating of the series hemichannel. GJ channel gates/sensors are presumed to be located in the pore where thy can sense V_j independent of V_m. Closure of one gate would largely collapse V_j across it, thereby changing V_j across the other series gate, so that the open probability of one gate depends on the state of the other through changes in the local field. Application of a negative voltage to one Cx46-expressing cell would tend to close the loop gate of the hemichannel in that cell, but would also tend to close the positive gate in the other Cx46 hemichannel. Closure of the positive gate would tend to keep the negative gate in the other hemichannel open. At steady state the channels cycle through different combinations of open/closed states, which would produce some residual conductance when the positive gate in one hemichannel is closed; closure of this gate leaves a residual conductance. The amount of residual conductance would be substantially less than that predicted by the ratio of open to subconductance states, as is the case here. This type of contingent interaction between series gates produces a similar result in Cx45 GJs (Bukauskas et al., 2002; Verselis and Bukauskas, 2003).

Effects of the D3N substitution

The simple expectation was that the D3N substitution would reverse the polarity of gating to substates in both Cx46 and

Cx50, producing hemichannels that show no evidence of closure at inside positive voltages. Although this was indeed the case, we could not determine whether gating polarity was reversed or gating was abolished. Gating between open and fully closed states predominated throughout the entire voltage range examined, obscuring other gating if present. In addition, the unitary conductances of Cx46 and Cx50 hemichannels were substantially reduced, by ~70% in both cases. Therefore, the D3N substitution has widespread effects on gating as well as on conductance. N-terminal residues have been found to be important in V_j gating as well as in the rectifying properties of GJ channels formed of Cx32 and Cx26, leading to the possibility that they contribute to the cytoplasmic vestibule of the pore (Verselis et al., 1994; Oh et al., 1999; Purnick et al., 2000a,b). Unfortunately, the D3C substitution in Cx46 caused loss of hemichannel function that precluded examination of its accessibility to cysteine-modifying reagents.

The significantly reduced unitary conductances of Cx46D3N and Cx50D3N hemichannels help explain the G–V_j relations of heterotypic GJs in which D3N containing hemichannels were paired to their wild-type counterparts. In all the heterotypic combinations examined, conductance increased from near zero at large V_j values relatively negative on the D3N side to reach a maximum at V_j values ~40–50 mV relatively positive on the D3N side, changes that can be attributed to loop gating of D3N hemichannels. At sufficiently large V_j values relatively positive on the D3N side, there are modest reductions in conductance that can be attributed to closure of the negative gates of wild-type Cx46 or Cx50 hemichannels. Why are the reductions in conductance attributed to the wild-type hemichannels modest? The reason is due to the small conductances of the D3N hemichannels compared to their wild-type counterparts. Since a GJ channel is composed of two hemichannels arranged in series, V_j represents the voltage drop along the entire length of the pore. If the two hemichannels differ in conductance, more of V_j will drop across the smaller conductance hemichannel, which in our case would be the D3N hemichannel. The effects are that the apparent V_j sensitivity of the D3N hemichannel increases, because it sees more voltage, and that of the series wild-type Cx46 or Cx50 hemichannel decreases, leading to dominance of the D3N hemichannel in the expression of V_j dependence. This phenomenon was first reported in heterotypic junctions containing Cx45, a connexin that makes a small conductance channel (Bukauskas et al., 2002).

In summary, this study demonstrates that individual properties of GJ channels can be explained by the behavior of the component hemichannels in two different connexins. These properties include unitary conductance, sensitivity to a selective pharmacological agent, and voltage gating. Taken together, these data indicate that there is substantial conservation of structure between unapposed hemichannels and GJ channels that encompasses many functional characteristics of connexins. In addition, we show that these two highly related connexins form hemichannels that have a multiplicity of voltage-gating mechanisms and, surprisingly, that GJ channels composed of these connexins primarily use different mechanisms to close in response to V_j. Thus, regulation of GJ-mediated communication by voltage can occur by different gating mechanisms, depending on the connexin isoform.

Both Cx46 and Cx50 are abundantly expressed in the lens. GJ-mediated communication is proposed to be an important component of the circulating current essential for maintenance of lens homeostasis (Mathias et al., 1997; Gao et al., 2004). This current is primarily carried by Na^+ ions that flow into fiber cells from the extracellular space, perhaps via hemichannels (Eckert et al., 1998), and then flows intercellularly via GJs back to the lens surface. The voltage-gating properties of Cx46 and Cx50, particularly those of the hemichannels, likely play a role in regulating this current.

We thank Angele Bukauskiene for technical assistance in preparation of *Xenopus* oocytes and Dr. Thomas White for providing the mouse Cx50 clone.

This work was supported by National Institutes of Health grants No. EY13869 to M.S. and No. GM54179 to V.K.V.

REFERENCES

Banach, K., and R. Weingart. 2000. Voltage gating of Cx43 gap junction channels involves fast and slow current transitions. *Pflugers Arch.* 439: 248–250.

Beahm, D. L., and J. E. Hall. 2002. Hemichannel and junctional properties of connexin 50. *Biophys. J.* 82:2016–2031.

Bukauskas, F. F., and R. Weingart. 1994. Voltage-dependent gating of single gap junction channels in an insect cell line. *Biophys. J.* 67: 613–625.

Bukauskas, F. F., A. Bukauskiene, M. V. Bennett, and V. K. Verselis. 2001. Gating properties of gap junction channels assembled from connexin 43 and connexin 43 fused with green fluorescent protein. *Biophys. J.* 81:137–152.

Bukauskas, F. F., A. B. Angele, V. K. Verselis, and M. V. Bennett. 2002. Coupling asymmetry of heterotypic connexin 45/connexin 43-EGFP gap junctions: properties of fast and slow gating mechanisms. *Proc. Natl. Acad. Sci. USA.* 99:7113–7118.

Bukauskas, F. F., and V. K. Verselis. 2004. Gap junction channel gating. *Biochim. Biophys. Acta.* 1662:42–60.

Contreras, J. E., F. F. Bukauskas, and M. V. Bennett. 2003. Gating and regulation of connexin 43 cx43 hemichannels. *Proc. Natl. Acad. Sci. USA.* 100:11388–11393.

Cruikshank, S. J., M. Hopperstad, M. Younger, B. W. Connors, D. C. Spray, and M. Srinivas. 2004. Potent block of Cx36 and Cx50 gap junction channels by mefloquine. *Proc. Natl. Acad. Sci. USA.* 101: 12364–12369.

Ebihara, L., and E. Steiner. 1993. Properties of a nonjunctional current expressed from a rat connexin 46 cDNA in *Xenopus* oocytes. *J. Gen. Physiol.* 102:59–74.

Ebihara, L., V. M. Berthoud, and E. C. Beyer. 1995. Distinct behavior of connexin 56 and connexin 46 gap junctional channels can be predicted from the behavior of their hemi-gap-junctional channels. *Biophys. J.* 68:1796–1803.

Eckert, R., P. Donaldson, K. Goldie, and J. Kistler. 1998. A distinct membrane current in rat lens fiber cells isolated under calcium-free conditions. *Invest. Opthalmol. Vis. Sci.* 39:1280–1285.

Eskandari, S., G. A. Zampighi, D. W. Leung, E. M. Wright, and D. D. Loo. 2002. Inhibition of gap junction hemichannels by chloride channel blockers. *J. Membr. Biol.* 185:93–102.

Gao, J., X. Sun, F. J. Martinez-Wittingham, X. Gong, T. W. White, and R. T. Mathias. 2004. Connections between connexins, calcium and cataracts in the lens. *J. Gen. Physiol.* 124:289–300.

Harris, A. L. 2001. Emerging issues of connexin channels: biophysics fills the gap. *Quart. Rev. Biophys.* 34:325–472.

Hopperstad, M. G., M. Srinivas, and D. C. Spray. 2000. Properties of gap junction channels formed by Cx46 alone and in combination with Cx50. *Biophys. J.* 79:1954–1966.

Kronengold, J., E. B. Trexler, F. F. Bukauskas, T. A. Bargiello, and V. K. Verselis. 2003. Single-channel SCAM identifies pore-lining residues in the first extracellular loop and first transmembrane domains of Cx46 hemichannels. *J. Gen. Physiol.* 122:389–405.

Mathias, R. T., J. L. Rae, and G. J. Baldo. 1997. Physiological properties of the normal lens. *Physiol. Rev.* 77:21–50.

Oh, S., J. B. Rubin, M. V. Bennett, V. K. Verselis, and T. A. Bargiello. 1999. Molecular determinants of electrical rectification of single channel conductance in gap junctions formed by connexins 26 and 32. *J. Gen. Physiol.* 114:339–364.

Oh, S., C. K. Abrams, V. K. Verselis, and T. A. Bargiello. 2000. Stoichiometry of transjunctional voltage-gating polarity reversal by a negative charge substitution in the amino terminus of a connexin 32 chimera. *J. Gen. Physiol.* 116:13–31.

Oh, S., S. Rivkin, Q. Tang, V. K. Verselis, and T. A. Bargiello. 2004. Determinants of gating polarity of a connexin 32 hemichannel. *Biophys. J.* 87:912–928.

Paul, D. L., L. Ebihara, L. J. Takemoto, K. I. Swenson, and D. A. Goodenough. 1991. Connexin 46, a novel lens gap junction protein, induces voltage-gated currents in nonjunctional plasma membrane of *Xenopus* oocytes. *J. Cell Biol.* 115:1077–1089.

Pfahnl, A., and G. Dahl. 1999. Gating of Cx46 gap junction hemichannels by calcium and voltage. *Pflugers Arch.* 437:345–353.

Purnick, P. E., D. C. Benjamin, V. K. Verselis, T. A. Bargiello, and T. L. Dowd. 2000a. Structure of the amino terminus of a gap junction protein. *Arch. Biochem. Biophys.* 381:181–190.

Purnick, P. E., S. Oh, C. K. Abrams, V. K. Verselis, and T. A. Bargiello. 2000b. Reversal of the gating polarity of gap junctions by negative charge substitutions in the N-terminus of connexin 32. *Biophys. J.* 79: 2403–2415.

Rubin, J. B., V. K. Verselis, M. V. Bennett, and T. A. Bargiello. 1992. Molecular analysis of voltage dependence of heterotypic gap junctions formed by connexins 26 and 32. *Biophys. J.* 62:183–193.

Srinivas, M., M. Costa, Y. Gao, A. Fort, G. I. Fishman, and D. C. Spray. 1999. Voltage dependence of macroscopic and unitary currents of gap junction channels formed by mouse connexin 50 expressed in rat neuroblastoma cells. *J. Physiol. (Lond).* 517:673–689.

Srinivas, M., M. G. Hopperstad, and D. C. Spray. 2001. Quinine blocks specific gap junction channel subtypes. *Proc. Natl. Acad. Sci. USA.* 98:10942–10947.

Trexler, E. B., M. V. Bennett, T. A. Bargiello, and V. K. Verselis. 1996. Voltage gating and permeation in a gap junction hemichannel. *Proc. Natl. Acad. Sci. USA.* 93:5836–5841.

Trexler, E. B., F. F. Bukauskas, J. Kronengold, T. A. Bargiello, and V. K. Verselis. 2000. The first extracellular loop domain is a major determinant of charge selectivity in connexin 46 channels. *Biophys. J.* 79:3036–3051.

Trexler, E. B., and V. K. Verselis. 2001. The study of connexin hemichannels (connexins) in *Xenopus* oocytes. *Methods Mol. Biol.* 154: 341–355.

Valiunas, V., and R. Weingart. 2000. Electrical properties of gap junction hemichannels identified in transfected HeLa cells. *Pflugers Arch.* 440:366–379.

Verselis, V. K., C. S. Ginter, and T. A. Bargiello. 1994. Opposite voltage gating polarities of two closely related connexins. *Nature.* 368:348–351.

Verselis, V. K., and F. F. Bukauskas. 2003. Connexin-GFPs shed light on regulation of cell-cell communication by gap junctions. *Curr. Drug Targets.* 3:489–499.

White, T. W., R. Bruzzone, D. A. Goodenough, and D. L. Paul. 1994. Voltage gating of connexins. *Nature.* 371:208–209.

White, T. W., D. L. Paul, D. A. Goodenough, and R. Bruzzone. 1995. Functional analysis of selective interactions among rodent connexins. *Mol. Biol. Cell.* 6:459–470.

White, T. W., M. R. Deans, O. B. J. M. R. Al-Ubaidi, D. A. Goodenough, H. Ripps, and R. Bruzzone. 1999. Functional characteristics of skate connexin 35, a member of the gamma subfamily of connexins expressed in the vertebrate retina. *Eur. J. Neurosci.* 11:1883–1890.

Wilders, R., and H. J. Jongsma. 1992. Limitations of the dual voltage-clamp method in assaying conductance and kinetics of gap junction channels. *Biophys. J.* 63:942–953.

Xu, X., V. M. Berthoud, E. C. Beyer, and L. Ebihara. 2002. Functional role of the carboxyl terminal domain of human connexin 50 in gap junctional channels. *J. Membr. Biol.* 186:101–112.

Zampighi, G. A., D. D. Loo, M. Kreman, S. Eskandari, and E. M. Wright. 1999. Functional and morphological correlates of connexin 50 expressed in *Xenopus laevis* oocytes. *J. Gen. Physiol.* 113:507–524.